Characterizing Febrile Seizure Susceptibility in *Scn1b* $^{+/-}$ Mice:

A Model for Genetic Epilepsy with Febrile Seizures Plus

by

Amanda Livia Kleeman

A Thesis Submitted in Partial Fulfillment of the

Requirements of the Degree of Bachelor of Arts

with Honors in Brain, Behavior, and Cognitive Science from the

University of Michigan

2012

Advisor: Dr. Lique Coolen

Principal Investigator: Dr. Lori Isom

Abstract

Genetic Epilepsy with Febrile Seizures Plus (GEFS+) is an autosomal disorder caused by mutations in α and β subunits of voltage gated sodium channels (VGSC) and gamma-aminobutyric acid (GABA) receptor channels. GEFS+ is associated with numerous epilepsy phenotypes, with febrile seizures starting in the first year of life being its most common feature. We predicted that mice with 50% of functional β1 subunits (*Scn1b*$^{+/-}$) would represent a model for GEFS+ by demonstrating heightened febrile seizure susceptibility compared to wildtypes (*Scn1b*$^{+/+}$). P15-16 *Scn1b*$^{+/-}$ mice demonstrated seizures of greater severity and seized earlier in the experimental period than *Scn1b*$^{+/-}$ mice, suggesting an age-specific onset of febrile seizure susceptibility. *Scn1b*$^{+/-}$ mice also exhibit a similar phenotype in seizure severity compared to preliminary data of P15-16 *Scn1b*$^{c/w}$ mice that have a heterozygous knock-in mutation *Scn1b-C121W*.

Keywords: epilepsy, voltage gated sodium channels, β subunits

Characterizing Febrile Seizure Susceptibility in *Scn1b* $^{+/-}$ Mice:

A Model for Genetic Epilepsy with Febrile Seizures Plus

Epilepsy is a neurological disorder characterized by repeated seizures over time and is caused by abnormal electrical activity in a population of neurons in the central nervous system (CNS) (Hauser, Annergers, & Kurland, 1993). Seizures vary broadly in both symptoms and severity depending on the area of the brain affected. Some seizures may cause minor staring spells in an individual, whereas others can cause brief blackouts, drooling or frothing from the mouth, teeth clenching, and uncontrollable muscle spasms. The symptoms can last anywhere from seconds to hours (A.D.A.M., Inc., 2011).

Epilepsy is the third most common neurological disorder in the U.S. and affects nearly 3 million Americans and 50 million people worldwid**e** (Epilepsy Foundation, 2010). About 40% of epilepsy patients develop seizures before the age of 16, and about 20% of patients after the age of 65 (Shorvon et al., 2009). Epilepsy can be acquired through a brain injury or spontaneous in origin, also known as an Idiopathic Generalized Epilepsy. Idiopathic epilepsies account for 20% of all patients with epilepsy. There are several subdivisions of idiopathic epilepsies, with a portion of them caused by mutations in voltage-gated or ligand-gated ion channels in the brain (Shorvon et al., 2009).

The types of seizures that occur most frequently during epilepsy are absence, myoclonic, and tonic-clonic seizures. Absence seizures usually occur during childhood and are characterized by a momentary loss of consciousness lasting 3-15 s. Myoclonic seizures, which begin in adolescence and persist through adulthood, are categorized by sudden, brief, arrhythmic jerks.

Finally, tonic-clonic seizures, also known as grand-mal seizures, cause rhythmic jerking of the extremities for ~30-40 s and loss of consciousness. Tonic-clonic seizures are the most frequent symptom of epilepsy leading to hospitalization (Mattson, 2003). Due to the complex heterogeneity of epilepsy mutations, it is difficult to match the exact pathophysiological mechanism of the patient with anti-epileptic drugs that can target specific ion channels or a combination of channels. As a result, 30% of patients with idiopathic epilepsies do not respond to pharmacological treatments to control their seizures (Heron, Scheffer, Berkovic, Dibbens, & Mulley, 2007). Due to such limited treatment options, epilepsy is a pervasive disorder that takes a large toll on patients' school achievements, employment opportunities, and everyday life experiences (Epilepsy Foundation, 2012).

Despite the limited success of anti-epileptic drugs in the treatment of idiopathic genetic epilepsies, research has uncovered an increasing number of voltage- and ligand-gated channel genes in which mutations disrupt normal neuronal activity. In particular, genes and susceptibility loci for idiopathic genetic epilepsies have been identified in gamma-aminobutyric acid (GABA) and acetylcholine receptor channels, and in voltage-gated calcium (Ca+), potassium (K+), and sodium (Na+) ion channels (Heron et al, 2007). The Isom Laboratory at the University of Michigan Medical School focuses on a specific class of idiopathic epilepsies called Genetic Epilepsy with Febrile Seizures Plus (GEFS+), which are caused by mutations in the genes encoding voltage-gated sodium channel β and α subunits as well as GABA receptor channels (Intractable Childhood Epilepsy Alliance, 2012).

GEFS+ is a wide spectrum of epileptic disorders ranging from the mild epilepsy of febrile seizure plus to its most severe form, Dravet Syndrome, a severe myoclonic epilepsy of infancy (Escayg & Goldin, 2010). GEFS+ has wide variations in its phenotype with its most common

feature being febrile seizures, or seizures precipitated by fever found usually in children. Dravet Syndrome is a rare genetic disorder that occurs in about 1 in 30,000 live births (Dravet Syndrome Foundation, 2012). Dravet Syndrome seizures usually begin during the first year of life and are frequently initiated by febrile seizures. Febrile seizures eventually lead to more serious tonic clonic or hemiclonic seizures, where only one side of the body is convulsive. Patients whose seizures last more than 30 minutes or occur in persistent clusters go into a state called status epilepticus and are in need of emergency medical attention (Intractable Childhood Epilepsy Alliance, 2012). In addition, Dravet Syndrome leads to a myriad of comorbidities including developmental delay, cognitive decline, ataxia, sleeping difficulties, chronic upper respiratory infections, sensory integration disorders, and disruptions of the autonomic nervous system. Dravet Syndrome patients also have a high incidence of sudden unexplained death in epilepsy (SUDEP), which may be caused by cardiac arrhythmia or autonomic dysfunction. Dravet Syndrome patients are usually pharmacoresistent to, or their symptoms are exacerbated by, traditional anti-epileptic drugs. Due to limited treatment options, patients face a diminished quality of life and are in need of constant supervision and care (Dravet Syndrome Foundation, 2012). Their prognosis is poor and early death, severe mental retardation, and institutionalization is common to many cases (Shorvon et al., 2009).

As mentioned earlier, Dravet Syndrome is the most rare and severe disorder on the GEFS+ spectrum. This research focuses specifically on the originally defined GEFS+ syndrome, a milder and much more common form of epilepsy in the currently defined GEFS+ spectrum. GEFS+ syndrome is an autosomal disorder associated with numerous epilepsy phenotypes. Patients suffer from febrile seizures beyond six years of age or exhibit afebrile generalized tonic-clonic seizures (Meisler & Kearney, 2005). Current research is slowly unraveling the genes

encoding genetic mutations in Na^+ channel α and β subunits and GABA receptors underlying GEFS+ syndrome in hopes of developing effective anti-epileptic drugs for this complex genetic epilepsy.

Voltage-Gated Na+ Channel Structure & Function

Voltage-gated Na+ channels (VGCS) are responsible for the rising phase of the action potential in the membranes of neurons and other electrically excitable cells such as cardiac and skeletal muscle myocytes (Isom, 2001). In response to a depolarizing stimulus, VGSCs are activated by undergoing a conformational change that increases their permeability to Na^+. As a result, Na^+ flows down its concentration gradient into the cell to depolarize the plasma membrane and initiate the action potential. VGSC inactivation (a state in which VGSCs no longer conduct ions), is concomitant with the opening of K^+ channels and results in action potential repolarization. In this state, the cell membrane hyperpolarizes before returning to its resting membrane potential (Escayg & Goldlin, 2010).

The structure of VGSCs is essential to their function. VGSCs are heterotrimers comprised of one α subunit and two β subunits. The α subunit is a highly processed ~260-kDa transmembrane protein made up of four tethered homologous domains (I-IV) that come together in pseudotetrafold symmetry to form the ion-conducting pore. Each of the four homologous domains contains six α-helical transmembrane segments called S1-S6 (Catterall, 2000) to total 24 transmembrane segments. Each of the four S4 segments acts as a voltage-sensor; upon sensing a small depolarization in the plasma membrane, they induce a conformational change of the VGSC pore into the open state to facilitate further membrane depolarization. The VGSC intracellular loop between domains III and IV is known as the inactivation gate. This domain

swings shut in a voltage-dependent manner to occlude the pore and prevent additional Na^+ from flowing through the channel (Escayg & Goldin, 2010).

Although the α subunit is sufficient for functional expression of Na^+ currents in heterologous systems, the β subunits are necessary for normal kinetics and voltage dependence of gating (Isom et al., 1992). Within the CNS, VGSCs are associated non-covalently with β1 or β3 subunits and covalently, through intermolecular disulfide bonds, with β2 or β4 subunits, resulting in a heterotrimer. All four β subunits are type I transmembrane proteins, consisting of a single transmembrane segment, an extracellular N-terminal signal peptide and immunoglobulin (Ig) loop domain, and an intracellular C-terminus. The Ig loop in the extracellular domain of each β subunit consists of an Ig fold of β sheets held together by hydrophobic interactions and a single intramolecular disulfide bond (Catterall, 2000). It is also important to note that the gene encoding for β1, *SCN1B*, encodes a splice variant called β1B, encoded by exons 1-3 with subsequent read-through of intron 3 that contains a termination codon and polyadenylation site (Kazen-gillespie et al., 2000). Although β1and β1B share the Ig loop domain, β1B lacks a transmembrane domain and is instead secreted into the extracellular medium (Brackenbury & Isom, 2011; Patino et al., 2011)

One of the most vital roles of β subunits consists of maintaining the normal kinetics and gating properties of VGSC. When β subunits are absent or dysfunctional cellular excitability can be significantly altered. For example, when VGSC β subunits are expressed without β subunits in *Xenopus* oocytes and mammalian fibroblasts, their Na^+ currents have a lower density, slower rates of inactivation, and a right-shifted voltage-dependence compared to Na^+ currents in control cells. The cells regain their normal properties when β subunits are restored (Isom, De Jongh, & Catterall, 1994).

Furthermore, isolated hippocampal pyramidal and bipolar neurons and cerebellar granule neurons lacking β1/β1B subunits (*Scn1b*$^{-/-}$) demonstrate subtle alteration in Na^+ current that have significant effects *in vivo*. *Scn1b*$^{-/-}$ CA3 hippocampal neurons exhibit a heightened peak voltage during action potential firing compared to wildtype (WT) neurons, while action potential firing is reduced in *Scn1b*$^{-/-}$ inhibitory cerebellar granule neurons (Brackenbury et al., 2010; Patino et al., 2009). In vivo, these combined effects can translate into major effects on cellular excitability. *Scn1b* null (*Scn1b*$^{/-}$) mice are a model of Dravet Syndrome that suffer from ataxia and frequent bilateral myoclonic seizures from postnatal day (P) 8-10 (Chen et al., 2004). They also have growth retardation, cardiac abnormalities (long QT syndrome), and experience death by P21(Patino et al., 2009).

Importantly, the physiological role of VGSC β subunits extends far beyond maintaining normal channel kinetics and gating modulation. β1 and β2 subunits function in cell-cell adhesion, cellular migration, regulation of neuronal patterning, and modulation of VGSC expression (Patino & Isom, 2010). In addition, the extracellular Ig loop of β 1is shown to be involved in α subunit interactions and cell adhesion, while its intracellular C- terminus is involved in ankyrin recruitment and cytoskeletal interactions (Isom, 2001). Furthermore, the secreted splice variant of *SCN1B*, β1B, is a cellular adhesion molecule that plays a role in embryonic development and promotes neurite outgrowth (Patino & Isom, 2010).

Mutations Associated with Dravet Syndrome.

Mutations in the gene encoding for the VGSC α subunit Nav1.1, *SCN1A*, are responsible for the majority of Dravet Syndrome and GEFS+ cases. Mammalian VGSC α subunits are encoded by nine genes, termed *SCN1A*-*SCN11A*. Of these nine isoforms, four are expressed

predominately in the CNS: Nav 1.1, Nav 1.2, Nav 1.3, and Nav 1.6. Mutations in *SCN1A*, encoding Nav1.1, account for approximately 10% of all GEFS+ cases and mutations or deletions in this gene account for about 70% of Dravet Syndrome cases (Lossin, 2009). Nav1.1 is located in the caudal regions of the adult brain, especially in the spinal cord (Beckh, Noda, Lübbert, & Numa, 1989; Gordon et al., 1987). It is predominantly found within the axon initial segments of parvalbumin-positive inhibitory interneurons of the developing neocortex and hippocampus where it regulates the release of the inhibitory neurotransmitter GABA. Lowered levels of Nav1.1 in PV alters the function of inhibitory circuits, and has been postulated to be the main cause of epileptic seizures in a mouse model of Dravet Syndrome with a loss of function nonsense mutation in *SCN1A* (Ogiwara et al., 2007).

Overall, over 600 mutations in *SCN1A* resulting in altered Nav1.1 activity are associated with Dravet Syndrome, which include a variety frame-shift, nonsense, and splice-site mutations Two functional SCN1A alleles are required for normal brain function, and thus patients who have a heterozygous mutation in *SCN1A* resulting in haploinsufficiency have an increased likelihood of developing Dravet Syndrome. Likewise, about 30 *SCN1A* mutations have been identified as a cause of the more benign GEFS+, all of which are missense mutations that result in altered Nav1.1 activity (Lossin, 2009).

Although the bulk of GEFS+ and Dravet Syndrome patients have some form of a mutation in *SCN1A*, the identification of patients with mutations in the β subunits of VGSCs has become an especially intriguing line of research. The genes *SCN1B-SCN4B* code for five mammalian β subunits: β1, β1B, β2, β3, and β4 (Brackenbury & Isom, 2011). The first diagnosed patient with GEFS+ had a heterozygous mutation in *SCN1B* (Wallace et al., 2002). This mutation, called β1-C121W, causes a disruption in the disulfide bond maintaining the

extracellular Ig fold in the β1/β1B subunit by changing a crucial cysteine amino acid residue to a tryptophan (Meadows et al., 2002). Mammalian cell lines expressing β1-C121W show subtle differences in VGSC function compared to cells expressing wildtype β1, including a positive-shift in the voltage dependence of channel availability and a rundown of current during high-frequency channel activation (Lossin et al., 2002; Meadows et al., 2002). These modifications may be subtle enough to allow normal VSCS functioning in neurons expressing this mutant subunit *in vivo* under non-stress-related conditions. However, neurons are sensitive to environmental stressors, and a fever may be sufficient to cause electrophysiological changes that result in epileptic seizures. In addition, disruption of the disulfide bond in the Ig fold of the β1-C121W mutant is postulated to contribute to the GEFS+ phenotype by disrupting β1-β1 cell adhesive interactions that lead to association of β1 with the cytoskeletal protein ankyrin, and/or disruption of β1 association with extracellular matrix molecules such as tenascin, although the mechanism behind how this leads to epilepsy remains unclear (Meadows et al., 2002).

Follow-up experiments using recombinant adeno-associated viruses to express β1 WT or β1 C121W in mouse neurons *in vivo* showed that WT β1 subunits are concentrated at the axon initial segment of pyramidal neurons, while β1 C121W subunits are absent from this subcellular domain (Wimmer et al., 2010). Wimmer et al. (2010) then generated a heterozygous knock-in mouse strain carrying the *Scn1b* C121W mutation as a model for patients with GEFS+. These investigators proposed that, similar to studies with *Scn1b* null mice, a reduction in β1 expression at the axon initial segment in *SCN1B* C121W mice causes hyper-excitability in the pyramidal neurons, thus making them more susceptible to behavioral arrest and seizures compared to WT mice (Brackenbury et al., 2010; Wimmer et al., 2010). The data also suggested that the β1-C121W "loss of function" mutation may precipitate an ultimate "gain-of-function" phenotype by

altering the voltage-dependent properties of α subunits and lowering their action potential threshold (Wimmer et al., 2010). Similarly, using *Scn1b* null mice, Brackenbury et al. (2010) found that β1 is necessary for the localization of Nav1.6 to the axon initial segment of cerebellar granule neurons, regulation of resurgent Na+ current, and maintenance of repetitive, high-frequency firing.

As mentioned earlier, most cases of Dravet Syndrome are caused by mutations in *SCN1A*. However, a patient identified by Patino et al. (2009) revealed that mutations in *SCN1B* can also cause Dravet Syndrome. This patient was unique from most patients with *SCN1B* mutations because he carried two mutant *SCN1B* alleles, leading to a homozygous loss of *SCN1B* function. Until this patient was identified, all patients with *SCN1B* mutations were found to be heterozygous and suffered from the milder GEFS+ syndrome. This novel homozygous mutation, p.R125C, prevented the trafficking of β1 subunits to the cell surface, resulting in loss of function. In this patient, inheritance of two alleles of p.R125C resulted in complete loss of *SCN1B* function, similar to the situation in *Scn1b*$^{-/-}$ mice. Hippocampal slice recordings performed comparing *Scn1b* $^{+/+}$ and *Scn1b*$^{-/-}$ mice indicated that that *Scn1b*$^{-/-}$ mice fired action potentials with a higher peak voltage and amplitude compared to *Scn1b*$^{+/+}$ mice. The study concluded that the *SCN1B* p.R125C mutation is a functional null phenotype that results in brain hyperexcitability, increasing the likelihood of the development of epileptic seizures (Patino et al., 2009). Interestingly, *Scn1b*$^{+/-}$ mice did not have a heightened seizure susceptibility compared to WT mice in response to intraperitoneal adminstration of pentylenetetrazole, a GABA receptor antagonist. Taken together, these results suggested that one functional *SCN1B* allele is sufficient for the maintenance of normal electrical excitability.

Seizure Susceptibility in *Scn1a* $^{+/-}$ Mice and Basis for Testing Seizure Susceptibility in

Scn1b $^{+/-}$ Mice

Oakley et al. (2008) at the University of Washington tested age- and temperature-dependence of seizures in mice with a heterozygous deletion of *Scn1a*. *Scn1a*$^{+/-}$ mice are models of Dravet Syndrome patients with a heterozygous loss-of-function mutation in *SCN1A* resulting in haploinsufficiency When the mouse core body temperature was raised through a heat lamp, *Scn1a* $^{+/-}$ mice exhibited seizures while *Scn1a* $^{+/+}$ mice were unaffected. Interestingly, *Scn1a* $^{+/-}$ mice were observed to experience temperature-induced seizures after postnatal day (P) 20, but not earlier in development, suggesting that *Scn1a* $^{+/-}$ mice are only susceptible to heat-induced seizures during a critical time period. Their seizure susceptibility worsened as the mice aged, however, and they began to develop spontaneous seizures after P32 (Oakley, Kalume, Yu, Scheuer, & Catterall, 2009).

Despite the plethora of current literature on GEFS+, Dravet Syndrome, and other seizure-related pathologies, there remains a myriad of unanswered questions regarding the variability of GEFS+ phenotypes in patients with heterozygous *SCN1B* mutations. This research will build off the current literature on the importance of β1/β1B subunits in modulating brain excitability by testing the thermal seizure susceptibility of *Scn1b*$^{+/-}$ mice. These mice do not seize spontaneously and live normal life spans. In spite of the previous observation that *Scn1b*$^{+/-}$ mice do not exhibit increased susceptibility to pharmacologically induced seizures (Patino et al., 2009), we postulate that they may have a heightened susceptibility to febrile induced seizures and may therefore be a model of GEFS+. Thus, the aim of this project is to determine whether *Scn1b* $^{+/-}$mice are more susceptible to seizures than *Scn1b*$^{+/+}$ mice when their body temperature is elevated. Seizure susceptibility will be characterized using a controlled heat lamp apparatus by measuring the latency to first seizure and seizure severity using a modified Racine Scale. Mice

will be separated into four age categories to determine whether there are differences in seizure manifestation throughout postnatal development and into early adulthood. Since GEFS+ syndrome in human patients is mainly associated with febrile seizures in childhood that begin during the first year of life, it is predicted that *Scn1b*$^{+/-}$ mice may be the most susceptible to seizures in the earlier age groups compared to *Scn1b*$^{+/+}$ mice, with differences in seizure susceptibility between the age groups becoming less prominent as the mice age (Shorvon, Duncan, Koepp, Sander, & Smith, 2009).

In contrast to the stated hypothesis, Catterall et al. (2008), who measured seizure susceptibility in *Scn1a*$^{+/-}$ mice as a model for Dravet Syndrome, found that seizure onset occurred at P20-21 and increased in severity at age P30-46. However, although Dravet Syndrome and GEFS+ syndrome are related in their pathophysiology, the manifestations of the two diseases may diverge with age, as Dravet Syndrome patients continue to develop more severe seizures later in life and often suffer from intractable epilepsy, early death, and severe mental retardation (Shorvon et al., 2009). Thus, if *Scn1b*$^{+/-}$ mice seize earlier in the experimental period than *Scn1a*$^{+/-}$ mice and have seizures of greater severity during this time period than the other model, they may potentially represent a mouse model for GEFS+ patients who have only 50% of their functioning *SCN1B* alleles.

Comparing Seizure Susceptibility of *Scn1b*$^{+/-}$ to *Scn1b*$^{c/w}$ Mice

The data from *Scn1b*$^{+/-}$ and *Scn1b*$^{+/+}$ mice will be compared to preliminary results showing the seizure susceptibility of mice with the heterozygous knock-in mutation *Scn1b-C121W* (referred to as *Scn1b*$^{c/w}$ mice). As mentioned in the introduction, expression of this mutant β1 subunit, at least in the axon initial segment, is postulated to cause hyperexcitability in

excitatory pyramidal neurons and thus an increased risk of developing seizures associated with GEFS+ (Wimmer, et al., 2010). Larisa Kruger, a second year Ph.D. candidate in the Department of Pharmacology in our laboratory, has been conducting seizure susceptibility tests on *Scn1b*$^{c/w}$ mice using identical age groups and protocols as my experiments with *Scn1b*$^{+/-}$ mice. It is predicted that *Scn1b*$^{c/w}$ mice may show a gain of function phenotype that render them more susceptible to seizures than *Scn1b*$^{+/-}$ mice which have only 50% of functioning *Scn1b* alleles. It is also postulated that the control (WT) mice in each group will show very similar trends in seizure susceptibility since they are of a similar C57Bl/6 genetic background.

Method

Mouse Subjects

Scn1b$^{+/-}$ mice were generated by homologous recombination as described in Chen et al. (2004). PCR analysis of genomic DNA isolated from mouse tails to determine the genotype is also explained in Chen et al. (2004). Four age groups of *Scn1b*$^{+/+}$ and *Scn1b*$^{+/-}$ mice were used to test seizure susceptibility: P10-11, P15-16, P20-21, and P30-33. These age groups were chosen to represent different stages in juvenile mouse development. A minimum of 10 mice were tested for each genotype in each group, with minimum of 20 mice in each age category.

Scn1b$^{c/w}$ mice were generated by homologous recombination in mouse embryonic stem cells as described in Wimmer et al. (2010) and obtained from Dr. Steven Petrou at the University of Melbourne. Mice were tested within the following age groups: P15-16, P20-21, and P30-33. However, for this thesis, the P15-16 data set of *Scn1b*$^{c/w}$ mice was the only age group completed for preliminary analysis and comparison to *Scn1b*$^{+/-}$ mice.

When this project was initiated in October 2010, the genotype of each mouse was known prior to the experimental period. Mouse testing was conducted by the author and a Ph.D. student who has now graduated, Dr. Gustavo Patino. Upon his graduation in December 2010, the author performed all of the mouse experiments. The decision was made to blind the experiment in June 2011 to remove any observer bias. Of the 81 mice used in the data analysis, 51 were conducted blindly. Data from the P10-11 age group was not included in the analysis for reasons explained in the results.

Experimental Procedures

Protocol 1. This protocol has been used previously in the literature to measure febrile seizures (Racine, 1972) and thus was important for us to compare our mice to other mouse strains. Note, however, a modified protocol (Protocol 2) was added below to measure core body temperature at seizure onset.

*Equipment***.** Each mouse was placed in a cylindrical plexiglass container for the duration of the experiment. A heat lamp was situatd over the top of the plexiglass container to increase the temperature of the environment and subsequently the internal body temperature of the mouse. The lamp was attached to a Physitemp, TCAT-2DF animal temperature controller that was programmed by the experimenter**.** A mouse RET-4 Thermocouple Sensor, Type T, rectal probe was used to measure the internal body temperature of the mouse and was attached to the rodent temperature controller. The rectal probe was inserted through the mouse rectum and situated to the tail using tape. A hollow strip of plastic was then placed over the 2-3 inches of wire projecting from the mouse rectum in order to prevent the mouse from chewing and damaging the wire of the rectal probe.

*Elevation of core body temperature***.** Prior to the insertion of the rectal probe, mice were injected subcutaneously with 1 mL of sodium chloride (NaCl) solution using a 27 ½ G needle to prevent dehydration during the core body temperature elevation procedure. The mice underwent a 30 minute acclimation period in the plexiglass container where the lamp temperature was held at a constant 37.0°C to allow the mouse to acclimate to the new environment. The purpose of the acclimation period was to decrease the role of stress as a potential factor in seizure induction. Upon completion of the acclimation period, the temperature of the heat lamp was increased 0.5°C every two minutes until a total of 20 minutes was reached and the heat lamp temperature read 42.5°C. The plexiglass container was then held at a temperature of 42.5°C for 15 minutes until the completion of the experimental period (see Figure 1).

Observation period. Mice were monitored for normal behavioral activity during the 30 minute acclimation period. During the experimental period of core body temperature elevation, mice were observed closely for the onset of seizures. Three measures were recorded for the first seizure and each subsequent seizure of increasing severity: (1) Time into the experimental period (0:00- 35:00 minutes), (2) internal core body temperature of the mouse (°C), and (3) the severity of the seizure using a modified Racine Scale (see Table 1). A similar modified Racine Scale protocol was used to measure seizure susceptibility in Martin et al. (2007).

Post-experimental procedures. Mice were euthanized and weighed after the end of the experimental period. The tail and ear-tag of each mouse was removed and stored in a -80°C freezer in the case that the mouse needed to be re-genotyped.

Analysis of seizure susceptibility. Seizure susceptibility was analyzed using the following measures: (1) The relationship between genotype and the time of the first observed seizure and

(2) the relationship between genotype and the rating of the most severe seizure observed. Data were separated by age group to determine whether differences in the seizure susceptibility between the genotypes were developmentally regulated.

Software and statistics. Microsoft Excel 2010 was used for initial data input. IBM SPSS was used to conduct the following statistics: (1) A Univariate Analysis of Variance to determine the main effect of genotype on the rating of the most severe seizure observed, (2) An independent t-test to determine whether there was a significant difference between the means of the most severe seizure rating between two genotypes, (3) A logistical regression to calculate the odds ratio of exhibiting a seizure with a Racine rating of 5 or 6, and (4) A Kaplan-Meier Test expressed as a survival function to determine the probability of having a seizure throughout the duration of the temperature induction period. GraphPad Prism 5 was used to (1) generate dot graphs depicting the severity of most severe seizure for each individual mouse, (2) create a model of the experimental protocol, and (3) perform the Mann-Whitney test comparing seizure severity by age (these data sets exhibited non-Gaussian Distribution).

Protocol 2: Accelerated Febrile Seizure Induction. This modification of Protocol 1 was created by Dr. Jack Parent's laboratory in the University of Michigan Department of Neurology and adapted upon the completion of the original data set using Protocol 1. Protocol 2 was added to the experimental procedures because it was very difficult to accurately measure differences in core body temperature at the onset of first seizure using the conditions in Protocol 1. In Protocol 1, the majority of mice did not seize until at least 20 minutes into the experiment, after the heat lamp temperature had reached 42.5C°, thus eliminating any potential variability in the core body temperature of the mice at the time of first seizure.

The data set for this protocol consisted of the same age categories (excluding the P10-11 mice due to reasons explained in Results), with at least 10 mice representing each genotype in each age group. Protocol 2 used the same equipment as Protocol 1 but the procedure differed from Protocol 1 in the following ways: (1) The mice were acclimated for 10 minutes in the plexiglass environment, (2) their body temperature was raised 0.5C° every 30 seconds, and (3) the experiment was terminated as soon as the first seizure was observed (see Figure 2). All other pre- and post- experimental procedures remained identical to Protocol 1. Data analysis specifically focused on the core body temperature of the mouse at its first seizure. GraphPad Prism 5 was used to conduct the Mann-Whitney Test on the data and create dot graphs depicting differences in core body temperature between the genotypes at the onset of their first seizure.

Results

Exclusions from Data Set

All mice in the P10-11 age group were excluded from our data analysis. These mice consistently seized at the Racine Scale stage 5 to 6 regardless of genotype, with many of them reaching death before the end of the experimental period. It is postulated that mice at this age undergo neuronal and developmental changes that make them more susceptible to seizures when their core body temperature is increased, regardless of genotype.

There were also three mice in the P20-21 data set that died during the acclimation period or very early on in the experimental period. These mice did not appear to have any seizures before experiencing status epilepticus and died shortly after. It is believed that these mice may have suffered from sudden unexplained death in epilepsy (SUDEP), and did not represent an

accurate model for seizures caused by increased body temperature. Thus, these mice were also excluded from the analysis.

Analysis of Seizure Severity

Results from the Univariate Analysis of Variance indicated that genotype was the only main effect accounting for differences in seizure severity rating F (1, 75) = 7.822, p = 0.007. There was no main effect of age F (2, 75) = 0.072, p = 0.93 or interaction between genotype and age F (2, 75) = 1.22, p = 0.30.). *Scn1b*$^{+/-}$ mice (M = 2.70, SD = 2.41) exhibited higher grade seizures compared to *Scn1b*$^{+/+}$ mice **(**M = 1.29, SD = 1.77) (see Figure 3). The independent sample t-test indicated that the difference between the means was significant t (76.6) = 3.02, p = 0.003. Levene's Test for Equality of Variances did not allow assumption of equal variances (F = 10.48, p = 0.002).

The ratings for seizure severity within independent age groups were analyzed using the Mann-Whitney test. Within the P15-16 age group, *Scn1b*$^{+/-}$ mice (Mdn = 1.00, SD = 1.88) exhibited more severe seizures than *Scn1b* $^{+/+}$ mice (Mdn = 2.50, SD = 1.20), (U = 37.0, p = 0.009) (see Figure 4).

In contrast to P15-16 mice, the P20-21 age group did not differ significantly in seizure severity between *Scn1b*$^{+/-}$ (Mdn = 0.00, SD = 2.62) and *Scn1b*$^{+/+}$ mice (Mdn = 2.00, SD = 2.13), (U = 93.0, p = 0.94) (see Figure 5). Similarly, the P30-33 age group did not exhibit significant differences in seizure severity between *Scn1b*$^{+/-}$ (Mdn = 4.00, SD = 2.79) and *Scn1b*$^{+/+}$ mice (Mdn = 0.00, SD = 1.87), (U = 47.5, p = 0.13) (see Figure 6).

Overall, Fisher's Exact Test demonstrated that *Scn1b*$^{+/-}$ mice (45.16%) did not have a significantly higher probability of having a seizure of *any* severity compared to *Scn1b*$^{+/-}$ mice

(64.00%) (p = 0.11). Importantly, however, 36.00% of *Scn1b*$^{+/-}$ mice exhibited seizures of grade 5 or 6 compared to 9.68% of *Scn1b*$^{+/+}$ mice, and these results were significant according to Fisher's Exact Test (p=0.01).

Analysis of Latency of to First Seizure

The Kaplan-Meier test was used to compare the latency to first seizure between genotypes, which was defined as a survival function. *Scn1b*$^{+/-}$ mice had a greater probability of seizing earlier in the experimental period (M = 27.7 minutes, SE = 0.96) compared to *Scn1b*$^{+/+}$ mice (M = 31.5 minutes, SE = 1.07) (see Figure 7). The Mantel-Cox test indicated that the difference in the survival distribution between *Scn1b*$^{+/-}$ and *Scn1b*$^{+/+}$ mice was significant (X^2 = 4.28, df = 1**,** p = 0.039).

The survival functions were also determined for individual age groups. Within the P15-16 age group, *Scn1b*$^{+/-}$ mice had a greater probability of seizing earlier into the experimental period (M = 25.53 minutes, SE = 1.21) compared to *Scn1b*$^{+/+}$ mice (M = 30.16 minutes, SE = 1.80) (see Figure 8). The Mantel-Cox test indicated that difference in the survival function was significant (X^2 = 4.79, df = 1, p = 0.029).

The P20-21 age group did not show any significant difference in latency to first seizure between *Scn1b*$^{+/-}$ (M = 29.34 minutes, SE = 1.57) and *Scn1b*$^{+/+}$ mice (M = 30.71 minutes, SE = 2.25) (see Figure 9). The Mantel-Cox test confirmed that the survival function did not differ between the two groups (X^2 = 0.039, df = 1, p = 0.84).

Finally, mice aged P30-33 likewise did not exhibit any significant difference in latency to first seizure between *Scn1b*$^{+/-}$ (M = 28.11 minutes, SE = 2.19) and *Scn1b*$^{+/+}$ mice (M = 33.46

minutes, *SE* = 1.29) (see Figure 10). The Mantel-Cox test confirmed that the survival function did not differ between the two groups (X^2= 1.998, *df* = 1, *p* = 0.157).

Analysis of Core Body Temperature at Onset of First Seizure

The accelerated febrile seizure induction protocol (Protocol 2) allowed us to analyze differences in core body temperature elevation at the onset of the first seizure. *Scn1b*$^{+/-}$ mice (*Mdn* = 42.55°C, *SD* = 0.730) seized at a lower core body temperature than *Scn1b*$^{+/-}$ mice on average (*Mdn* = 42.05 °C, *SD* = 0.753) with a trend toward significance (*U* = 54.5, *p* = 0.057) (see Figure 11). However, a significant difference was found in core body temperature between *Scn1b*$^{+/+}$ (*Mdn* = 42.64 °C, *SD* = 0.730) and *Scn1b*$^{+/-}$ mice (*Mdn* = 42.00°C, *SD* = 0.522) when a the highest rated data point in the *Scn1b*$^{+/-}$ mouse group was removed from the data set (*U* = 39.0, *p* = 0.017) Although this point did not pass Grubbs' test for outliers (*Z* = 2.41, *p* > 0.05), a trend toward significance can be still suggested by the data. Additional febrile seizure experiments are needed to confirm these findings. Within the P20-P21 age group, there was no significant difference in core body temperature at onset of first seizure between *Scn1b*$^{+/+}$ (*Mdn*= 43.35°C, *SD*=0.914) and *Scn1b*$^{+/-}$ mice (*Mdn*= 43.20°C, *SD*=0.659) (*U*= 60.50, *p*=.804) (see Figure 12).

Seizure Severity of P15-16 *Scn1b*$^{c/w}$ Mice and Comparison with P15-16 *Scn1b*$^{+/-}$ Mice

Preliminary data suggest that, as expected from Wimmer, et al. (2010), P15-16 *Scn1b* $^{c/w}$ mice (*Mdn* = 5.00, *SD* = 2.29) exhibited seizures of greater severity than their WT counterparts, P15-16 *Scn1b*$^{c/c}$ mice (*Mdn*= 3.00, *SD* = 1.35), (*U* = 97.0, *p* = 0.026) (see Figure 13). For reasons that are not clear, *Scn1b* $^{c/c}$ mice exhibited seizures of greater severity than *Scn1b*$^{+/+}$ mice (*Mdn* = 1.00, *SD* =1.20) (*U* = 38.50, *p* = 0.023) (see Figure 14). Finally, *Scn1b*$^{c/w}$ mice and *Scn1b*$^{+/-}$ mice

(*Mdn* = 2.50, *SD* = 1.88) did not differ significantly in their seizure severity ratings ($U = 134.5$, $p = 0.12$) (see Figure 15*).*

Latency to First Seizure of P15-16 *Scn1b*$^{c/w}$ Mice and Comparison with *Scn1b*$^{+/-}$ Mice

The Kaplan-Meier test was used to compare the latency to first seizure between the *Scn1b*$^{+/+}$, *Scn1b*$^{-/-}$, *Scn1b*$^{c/w}$, and *Scn1b*$^{c/c}$ mice, which was expressed as a survival function. *Scn1b*$^{+/-}$ (*Mdn* = 24.09 minutes), *Scn1b*$^{c/c}$ (*Mdn* = 21.00 minutes), and *Scn1b*$^{c/w}$ (*Mdn* = 18.33 minutes) exhibited similar curves. *Scn1b*$^{+/+}$ mice (*Mdn* = 32.85 minutes) were the only group that seized later in the experimental period (see Figure 16). The Mantel Cox Test confirmed that this difference was significant ($X^2 = 9.41$, df = 1, $p = 0.024$).

Discussion

The results suggest that there is a difference in febrile seizure susceptibility between *Scn1b*$^{+/-}$ and *Scn1b*$^{+/+}$ mice. When the data were aggregated and analyzed as a whole, *Scn1b*$^{+/-}$ mice seized both earlier in the experimental period and exhibited more severe seizures on average compared with their WT littermates. However, when the data were analyzed separately according to age group, the trends in seizure susceptibility varied. In fact, the P15-16 age group was the only category that demonstrated a significant and prominent deviation in time to first seizure and seizure severity between *Scn1b*$^{+/-}$ and *Scn1b*$^{+/+}$ mice. The P20-21 and P30-33 age groups, on the other hand, exhibited little to no statistically significant differences in seizure susceptibility between genotypes. Although the data are not statistically significant, the graphs depicting the P20-21 and P30-33 mice illustrate that there is a trend towards *Scn1b*$^{+/-}$ mice seizing earlier in the experimental period and exhibiting more severe seizures than *Scn1b*$^{+/+}$ mice.

The results from the accelerated febrile seizure induction protocol (Protocol 2) revealed similar trends in the P15-16 age group regarding increased seizure susceptibility in the *Scn1b*$^{+/-}$ mice compared to WT. On average, *Scn1b*$^{+/+}$ core body temperature was higher than *Scn1b*$^{+/-}$ at the onset of the first observed seizure in P15-16 with a trend towards significance. However, *Scn1b*$^{+/-}$ and *Scn1b*$^{+/+}$ mice in the P20-21 group exhibited almost identical body temperatures on average at the onset of first seizure. As noted previously, it was difficult to accurately measure differences in core body temperature at the onset of first seizure using Protocol 1. Thus, these data indicate that core body temperature is another measurable variable that can be utilized to characterize seizure susceptibility. However, this data set is still incomplete. Mice in the P30-31 age groups are currently being tested using Protocol 2. Based on the results from Protocol 1, it is predicted that the difference in core body temperature at the onset of the first seizure between *Scn1b*$^{+/-}$ and *Scn1b*$^{+/+}$ mice will be likewise be non-significant in the P30-33 mice.

The differences in seizure susceptibility among the age groups varied from the original hypothesis. Seizure susceptibility peaked in the P15-16 mice, while differences in seizure susceptibility were not significant in either the P20-21 or P30-33 age groups. However, within the two older age categories, seizure susceptibility was more pronounced in *Scn1b*$^{+/-}$ P30-33 mice compared to *Scn1b* $^{+/-}$ P20-21 mice, which did not support the prediction that the seizures would decrease in severity with age.

The persistent and severe seizures of the P10-11 *Scn1b*$^{+/-}$ and *Scn1b*$^{+/+}$ mice can be explained by a heightened susceptibility to seizures at this stage of neuronal development. Human children are the most susceptible to febrile seizures at postnatal days 8-14 (Clancy, Darlington, & Finlay, 2001). In addition, van Gassen et al. (2008) used P10-14 mice to characterize febrile seizure susceptibility in several mouse inbred strains, and found that

behavioral analysis of seizures was the most reliable when mice were 10 days old. Thus, these mice were excluded from the data set because they are believed to be in the primary stages of neuronal development, which may have caused a heightened susceptibility to seizures in response to body temperature increases regardless of genotype.

In contrast to the P10-11 group, the manifestation of seizure susceptibility between *Scn1b*$^{+/-}$ and *Scn1b*$^{+/+}$ mice differentiated at P15-16. This age group may represent a model for the developmental onset of GEFS+ in human patients that are midway through the first year of life. Interestingly, the decrease in seizure susceptibility in *Scn1b*$^{+/-}$ compared to *Scn1b*$^{+/+}$ mice starting at P20 may be a result of the mice nearing the end of the critical period of postnatal brain development. Despite the data suggesting that *Scn1b*$^{+/-}$ mice have an age-specific febrile seizure susceptibility, we cannot conclusively say these mice are a true model for *SCN1B*-linked GEFS+ patients without more rigorous genetic and electrophysiological testing.

The results from this experiment differ from those reported by Oakley et al. (2008) who measured febrile seizure susceptibility of *Scn1a*$^{+/-}$ mice, a model of Dravet Syndrome. One unexpected contrast occurred in the P10-11 age group. Neither *Scn1a*$^{+/-}$ nor *Scn1a*$^{+/+}$mice from Oakley et al. (2008) experiments exhibited seizures at this age, whereas not P10-11 *Scn1b*$^{+/-}$ and *Scn1b*$^{+/+}$ mice observed the most pervasive and severe seizures compared to the older age groups. In addition, in *Scn1a*$^{+/-}$ mice febrile seizure onset occurred at P15-16 and peaked at P30-46. Conversely, differences in *Scn1b*$^{+/-}$ and *Scn1b*$^{+/+}$ seizure susceptibility peaked at P15-16 and declined starting at P20. Another interesting comparison was the difference in seizure susceptibility between *Scn1a*$^{+/+}$ and *Scn1b*$^{+/+}$ mice. Oakley et al. (2008) did not observe any seizures in *Scn1a*$^{+/+}$ mice across all age groups, whereas seizures in *Scn1b*$^{+/+}$ mice were prevalent across all age groups, with some *Scn1b*$^{+/+}$ mice exhibiting seizures with Racine ratings

as high as 5 or 6. Despite the similarity in genetic background (both cohorts were congenic on C57Bl/6), the strong contrasts in seizure susceptibility between *Scn1a*$^{+/-}$ and *Scn1b*$^{+/-}$ mice further suggest that GEFS+ syndrome and Dravet Syndrome may differ in their manifestations as the diseases progress with age. This may contribute to the large heterogeneity of symptoms associated with GEFS+ spectrum disorders, and may reflect the wide variations in VGSC membrane hyper-excitability caused by *SCN1A* and *SCN1B* mutations.

Comparing *Scn1b*$^{+/-}$ and *Scn1b*$^{c/w}$ Seizure Susceptibility

Although this data set is incomplete, a preliminary analysis of the seizure susceptibility of P15-16 *Scn1b*$^{c/c}$ and *Scn1b*$^{c/w}$ mice was performed to determine whether there were similar trends to the data observed comparing P15-16 *Scn1b*$^{+/+}$ and *Scn1b*$^{+/-}$ mice. As predicted, *Scn1b*$^{c/w}$ exhibited more severe seizures than *Scb1b*$^{c/c}$ mice. Importantly, there was no significant difference in seizure severity in *Sc1b*$^{c/w}$ compared to *Scn1b*$^{+/-}$ mice, suggesting that *SCN1B*-C121W may not be a gain of function mutation, at least in this behavioral assay. However, there was an unexpected significant difference between *Scn1b*$^{+/+}$ mice and. *Scn1b*$^{c/c}$ mice seizure severity, even though these mouse strains have similar C57Bl/6 genetic backgrounds. This difference may be a result of observer variability or underlying genetic differences that have yet to be investigated.

Finally, the survival function analysis depicting latency to first seizure provides contradicting results. Although *Scn1b*$^{c/w}$ mice exhibited more severe seizures than *Scn1b*$^{c/c}$ mice, the two genotypes had similar rates of overall seizure occurrence, with the first seizure being observed at similar times in the experimental period. In fact, of all four cohorts, the *Scn1b*$^{+/+}$ mice were the only group that had a significantly lower rate of seizure occurrence and longer

latency to first seizure. It is possible that latency to first seizure may not be an accurate method of characterizing differences in seizure susceptibility between *Scn1b*$^{c/w}$ and *Scn1b*$^{c/c}$ mice. Nonetheless, this comparison is only in its preliminary stages of analysis. More data need to be compiled from older age groups to determine whether differences in seizure susceptibility between *Scn1b*$^{c/w}$ and *Scn1b*$^{c/c}$ mice are specific to the P15-16 age range or extend into adulthood. In addition, the discrepancy in seizure severity between *Scn1b*$^{+/+}$ and *Scn1b*$^{c/c}$ mice is subject to further analysis. If it can be ascertained that there is a genetic difference in backgrounds between these two "WT" groups, our preliminary comparisons regarding *Scn1b*$^{+/-}$ and *Scn1b*$^{c/w}$ will likewise be affected by this confounding variable.

Future Directions

EEG Activity. Identifying P15-16 as a critical age period for phenotypic differences in seizure susceptibility provides a stepping-stone for future projects. In the experiment conducted by Oakley et al. (2008) on *Scn1a*$^{+/-}$ mice, seizure activity was recorded using video EEG where spike-and-wave discharge complexes in brain regions could be visualized. The EEG was also used to measure the epileptic activity between seizures (interictal activity), which is often used to clinically diagnose and characterize an epilepsy syndrome (Oakley et al., 2009). Although EEG is a more accurate measure of characterizing seizure susceptibility, the process is both costly and invasive. The results of these preliminary experiments have identified the P15-16 mice as promising candidates for EEG analysis to strengthen the findings regarding heightened seizure susceptibility in *Scn1b*$^{+/-}$ mice.

Neurite Outgrowth. VGSC β 1 subunits have also been shown to be involved in the modulation of axonal migration in developing cerebellular neurons (CGN). *Scn1b*$^{-/-}$ (null) mice

show pathfinding defects in the corticospinal tract, one of the last major developing fiber tracts that enter the spinal cord. Compared to *Scn1b*$^{+/+}$ mice, the axons in *Scn1b* nulls exhibit significant axonal defasciculation when migrating from the ventral pyramid of the hindbrain to the dorsal column of the rostral spinal cord (Brackenbury et al., 2008). Future experiments in the Isom Laboratory will observe neuronal migration in brain slices of *Scn1b*$^{+/-}$ and *Scn1b*$^{c/w}$ mice to quantify and compare the levels of axonal defasciculation caused by the expression of their respective β1 mutations.

Na^+ Current Density. The Isom Laboratory also plans to extract fibroblasts from patients with the *SCN1B* C121W mutation, which will be reprogrammed into induced pluripotent stem cells (iPSC). These iPSCs will be differentiated into neurons and used to measure Na^+ current density in comparison to *Scn1b* wildtypes.

Limitations of Experimental Design

The nature of this experimental design created limitations for interpretation. The most prominent limitation was the subjectivity of human observation. As explained in the legend in Figure 2, the rating of 1 on the Racine Scale was excluded due to the difficulty in identification of a seizure of such low grade. In addition, recording the time and grade of each seizure during the experimental period can vary based on the observer. This limitation could potentially serve as an extraneous variable when comparing seizure susceptibility in *Scn1b*$^{+/-}$ mice to *Scn1b*$^{c/w}$ mice, which were tested by Larissa Kruger.

Another main limitation of the study was the inability to analyze differences in core body temperature between the two genotypes using Protocol 1. Most mice did not seize until body temperature was raised to 42.5°C at 20 minutes into the experiment. Since this temperature was

held constant for the remainder of the experimental period, we were unable to determine whether body temperature was an important variable in measuring seizure susceptibility. However, with the adaptation of the accelerated febrile seizure induction protocol (Protocol 2), it was possible to address questions regarding core body temperature differences at the onset of the first seizure. Finally, there is the possibility that some mice experienced more stress than others during the experiment, which may have led to premature seizure or seizures of greater severity. Such stressors included the NaCl solution injection, rectal probe insertion, or the re-insertion of a probe during the experimental period.

References

A.D.A.M., Inc. (2011, March 28). *Epilepsy*. Retrieved from PubMed Health: http://www.ncbi.nlm.nih.gov/pubmedhealth/PMH0001714/

Beckh, S., Noda, M., Lübbert, H., & Numa, S. (1989). Differential regulation of three sodium channel messenger RNAs in the rat central nervous system during development. *The EMBO journal*, *8*(12), 3611-6. Retrieved from http://www.pubmedcentral.nih.gov/articlerender.fcgi?artid=402042&tool=pmcentrez&rendertype=abstract

Brackenbury, W. J., Davis, T. H., Chen, C., Slat, E. a, Detrow, M. J., Dickendesher, T. L., Ranscht, B., et al. (2008). Voltage-gated Na+ channel beta1 subunit-mediated neurite outgrowth requires Fyn kinase and contributes to postnatal CNS development in vivo. *The Journal of neuroscience : the official journal of the Society for Neuroscience*, *28*(12), 3246-56. doi:10.1523/JNEUROSCI.5446-07.2008

Brackenbury, W. J., & Isom, L. L. (2011, September). Na+ channel β subunits: overachievers of the ion channel family. *frontiers in Pharmacology, 2*.

Brackenbury, W. J., Jeffrey, D. C., Chunling, C., Miyazaki, H., Nukina, N., Oyama, F., . . . Isom, L. L. (2010, February 2). Functional reciprocity between Na+ channel Nav1.6 and β1 subunits in the coordinated regulation of excitability and neurite outgrowth. *Proceedings of the National Academy of the Sciences, 107*(5), 2283-2288.

Catterall, W. A. (2000, April). From ionic currents to molecular mechanims: the structure and function of voltage-gated sodium channels. *Neurons, 26*, 12-25.

Chen, C., Westenbroek, R. E., Xu, X., Sorenson, D. R., Chen, Y., McEwen, D. P., . . . Isom, L. L. (2004). Mice lacking sodium channel beta1 subunits display defects in neuronal excitability, sodium channel expression, and nodal architecture. *Journal of Neuroscience*, 4030-42.

Clancy, B., Darlington, R. B., & Finlay, B. L. (2001). Translating developmental time across mammalian species. *Neuroscience, 106*(1), 7-17.

Dravet Syndrome Foundation. (2012). *What is Dravet Syndrom*. Retrieved from Dravet Syndrome Foundation: http://www.dravetfoundation.org/dravet-syndrome/what-is-dravet-syndrome

Engel, J. (2001). *Clinical Summary: Genetic epilepsy with febrile seizures plus*. Retrieved from Neurology MedLink: http://www.medlink.com/medlinkcontent.asp

Epilepsy Foundation. (n.d.). *About Epilepsy*. Retrieved from Epilepsy Foundation: http://www.epilepsyfoundation.org/aboutepilepsy/

Escayg, A., & Goldin, A. L. (2010). Sodium channel SCN1A and epilepsy: mutations and mechanism. *Epilepsia, 51*(9), 1650-1658.

Escayg, A., & Goldlin, A. L. (2010). Sodium channel SCN1A and epilepsy: mutations and mechanisms. *Epilepsia, 51*(9), 1650-1658.

Gordon, D., Merrick, D., Auld, V., Dunn, R., Goldin, a L., Davidson, N., & Catterall, W. a. (1987). Tissue-specific expression of the RI and RII sodium channel subtypes. *Proceedings of the National Academy of Sciences of the United States of America*, *84*(23), 8682-6. Retrieved from

http://www.pubmedcentral.nih.gov/articlerender.fcgi?artid=299610&tool=pmcentrez&rendertype=abstract

Hauser, W. A., Annergers, J. F., & Kurland, L. T. (1993). Incidence of epilepsy and unprovoked seizures in Rochester, Minnesota: 1935-1984. *Epilepsia, 34*(3), 453-468.

Heron, S. E., Scheffer, I. E., Berkovic, S. F., Dibbens, L. M., & Mulley, J. C. (2007, April). Channelopathies in idiopathic epilepsy. *Neurotherapeutics, 4*(2), 295-304.

Intractable Childhood Epilepsy Alliance. (2012). *Understanding Dravet Syndrome*. Retrieved from http://www.ice-epilepsy.org/ice-informational-brochure.html

Isom, L. L. (2001). Sodium channel β Subunits: anything but auxiliary . *Neuroscientist, 42*(7), 42-54.

Isom, L. L., De Jongh, K. S., Patton, D. E., Reber, B. F., Offord, J., Charbonneau, H., . . . Catterall, W. A. (1992, May 8). Primary structure and functional expression of the B1 subunit of the rat brain sodium channel. *Science, 256*, 839-842.

Isom, L. L., De Jongh, S. K., & Catterall, W. A. (1994, June). Auxiliary subunits of voltage-gated ion channels. *Neuron, 12*, 1183-1194.

Kazen-gillespie, K. A., Ragsdale, D. S., Andrea, M. R. D., Mattei, L. N., Rogers, K. E., & Isom, L. L. (2000). Cloning , Localization , and Functional Expression of Sodium Channel ␣ 1A Subunits *. *Biochemistry*, *275*(2), 1079-1088.

Lossin, C. (2009, February). A catalog of SCN1A variants. *Brain Development, 31*(12), 114-130.

Lossin, C., Wang, D. W., Rhodes, T. H., Vanoye, C. G., & George, A. L. (2002). Molecular basis of an inherited epilepsy. *Neuron*, *34*(6), 877-84. Retrieved from http://www.ncbi.nlm.nih.gov/pubmed/12086636

Martin, M. S., Tang, B., Papale, A. L., Yu, H. F., Catterall, W. A., & Escayg, A. (2007, August 23). The voltage-gated sodium channel Scn8a is a genetic modifier of severe myoclonic epilepsy of infancy. *Human Molecular Genetics*, *16*(23), 2892-2899.

Mattson, R. H. (2003). Overview : Idiopathic Generalized Epilepsies. *Childhood A Global Journal Of Child Research*, *44*, 2-6.

Meadows, L. S., Malhotra, J., Loukas, A., Thyagarajan, V., Kazen-gillespie, K. A., Koopman, M. C., Kriegler, S., et al. (2002). Functional and Biochemical Analysis of a Sodium Channel ^{N_L} 1 Subunit Mutation Responsible for Generalized Epilepsy with Febrile Seizures Plus Type 1. *Analysis*, *22*(24), 10699-10709.

Meisler, M. H., & Kearney, J. A. (2005, August). Sodium channel mutations in epilepsy and other nuerological disorders. *The Journal of Clinical Investigations*, *115*(8), 2010-2017.

Oakley, J. C., Kalume, F., Yu, F. H., Scheuer, T., & Catterall, W. A. (2009, March 10). Temperature- and age-dependent seizures in a mouse model of severe myoclonic epilepsy in infancy. *PNAS*, *106*(10), 3994-3999.

Ogiwara, I., Miyamoto, H., Morita, N., Atapour, N., Mazaki, E., Inoue, I., Takeuchi, T., et al. (2007). Nav1.1 localizes to axons of parvalbumin-positive inhibitory interneurons: a circuit basis for epileptic seizures in mice carrying an Scn1a gene mutation. *The Journal of*

neuroscience : the official journal of the Society for Neuroscience, *27*(22), 5903-14. doi:10.1523/JNEUROSCI.5270-06.2007

Patino, G. a, Brackenbury, W. J., Bao, Y., Lopez-Santiago, L. F., O'Malley, H. a, Chen, C., Calhoun, J. D., et al. (2011). Voltage-gated Na+ channel β1B: a secreted cell adhesion molecule involved in human epilepsy. *The Journal of neuroscience : the official journal of the Society for Neuroscience*, *31*(41), 14577-91. doi:10.1523/JNEUROSCI.0361-11.2011

Patino, G. A., & Isom, L. L. (2010). Electrophysiology and beyonf: multiple roles of Na+ channel voltage-gated Na+ channels: potential for beta subunits as β subunits in development and disease. *Neuroscience Letters*.

Patino, G. a, Claes, L. R. F., Lopez-Santiago, L. F., Slat, E. a, Dondeti, R. S. R., Chen, C., O'Malley, H. a, et al. (2009). A functional null mutation of SCN1B in a patient with Dravet syndrome. *The Journal of neuroscience : the official journal of the Society for Neuroscience*, *29*(34), 10764-78. doi:10.1523/JNEUROSCI.2475-09.2009

Racine, R. (1972, March). Modification of seizure activity by electrical stimulatoin. *Electroencephalography and Clinical Neurophysiology*, *32*(3), 281-294.

Shorvon, S., Duncan, J., Koepp, M., Sander, J., Smith, S., & Walker, M. (2009). Epilepsy and Related Disorders. In *Neurology: A Queen Square Textbook* (pp. 189-243). Blackwell Publishing Ltd.

van Gassen, K. L. I., Hessel, E. V. S., Ramakers, G. M. J., Notenboom, R. G. E., Wolterink-Donselaar, I. G., Brakkee, J. H., Godschalk, T. C., et al. (2008). Characterization of febrile

seizures and febrile seizure susceptibility in mouse inbred strains. *Genes, brain, and behavior*, *7*(5), 578-86. doi:10.1111/j.1601-183X.2008.00393.x

Wallace, R.H, Scheffer, I.E, Parasivam, G., Barnett, S., Wallace, G.B., Sutherland G.R., Berkovic, S.F., Mulley, J. C. (2002). seizures plus : *Neurology*, 2000-2003.

Wimmer, V. C., Reid, C. A., Mitchell, S., Richards, K. L., Scaf, B. B., Leaw, B. T., . . . Petrou, S. (2010, August). Axon initial segment dysfunction in a mouse model of genetic epilepsy with febrile seizure plus. *The Journal of Clinical Investigation*, *120*, 2661-2671.

Author Note

My thesis is a culmination of my research in the Isom Laboratory I have called home for the past two years. Compiling this project has been an incredibly rewarding experience that would not have been made possible without this talented and supportive family of scientists that drive the continued success of the Isom Laboratory.

This project was the brainchild of Dr. Gustavo Patino, Neuroscience Ph.D. graduate and my first mentor in the biomedical science who influenced my desire to write this thesis. Thank you for teaching me the basics of lab work, never ceasing to challenge me, and your continued support during your time in Columbia. I welcome you back to the UM family! Jeff and Chunling, thank you for your everyday support in helping me run my experiments and showing such patience in explaining concepts and answers to my questions. Larissa, thank you for all your invaluable help in consolidating information and giving me insight on how to analyze my results. I am very grateful for the opportunity to collaborate our data and incorporate the preliminary stages of your work into my thesis. I look forward to hearing about your future results! Finally, Lori, I am so grateful to have had this opportunity to work in your lab these past two years. You have provided me with endless guidance and a nurturing environment for me to grow and learn as a researcher. I could not have envisioned a better lab for an undergraduate to explore and appreciate the science of pharmacology. I have learned an unimaginable amount not just about research, but about perseverance, work ethic, being challenged and having patience.

After I graduate, I will to miss coming to the lab every week as it has become one of the most integral part of my undergraduate experience. I wish everyone the best of luck in their future research endeavors, and I will always hold fond memories of the Isom Lab in remembering my four unforgettable years at the University of Michigan.

Table 1:

The Modified Racine Scale

Racine Score	Description
0	No response
1	Staring, unresponsive
2	Focal/clonic convulsion (head nod, twitch, myoclonic jerk, backing)
3	Forelimb clonus (tonic/clonic seizures)
4	Rearing
5	Loss of posture (jumping, rearing, falling)
6	Status epilepticus, death

The Modified Racine Scale was used to categorize seizure severity during the experimental period (Martin, et al., 2007, Racine, 1972). For the purpose of this experiment, a seizure rating of 1 was not recorded in the data due to subjectivity in recognizing such a low-grade seizure. Thus, only seizures with a minimum grade of 2 were recorded and included in the data analysis.

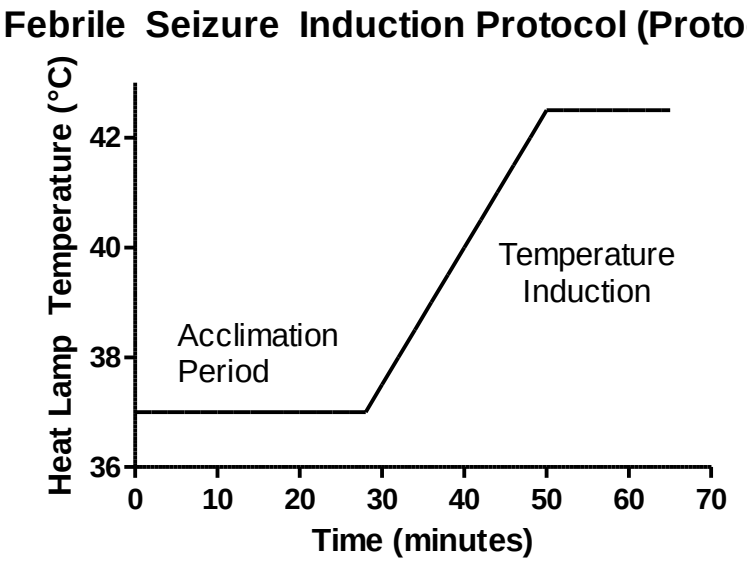

Figure 1. Febrile Seizure Induction Protocol (Protocol 1). Mice were acclimated for 30 minutes at 37°C. During the experimental period, the lamp temperature was raised 0.5°C every 2 minutes until 42.5°C. The mice were then held at a temperature of 42.5°C for an additional 15 minutes.

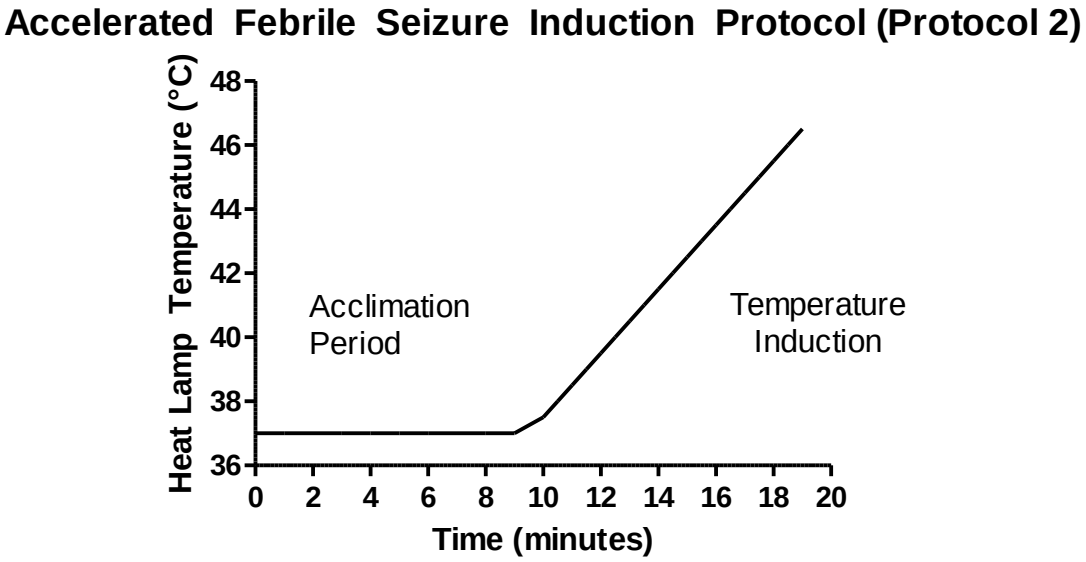

Figure 2. Accelerated Febrile Seizure Induction Protocol (Protocol 2). Mice were acclimated for 10 minutes at 37°C. During the experimental period, the lamp temperature was raised .5°C every 30 seconds until the mouse seized.

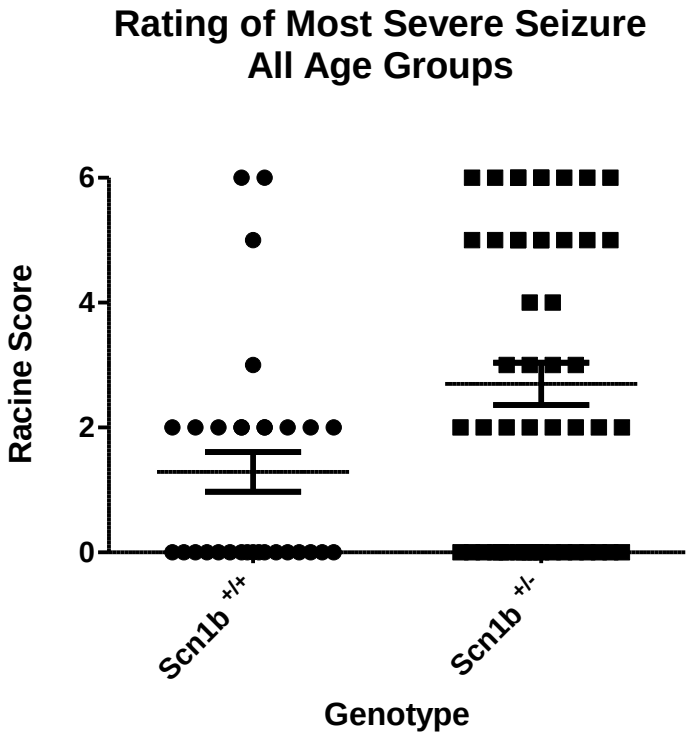

Figure 3: The ratings of most severe seizures observed in *Scn1b*$^{+/-}$ (*n* = 50) and *Scn1b*$^{+/+}$ mice (*n* = 31). *Scn1b*$^{+/-}$mice (*M* = 2.70, *SD* = 2.41) exhibited higher grade seizures compared to *Scn1b*$^{+/+}$ mice **(***M* = 1.29, *SD* = 1.77). The independent sample t-test indicated that the difference between the means was significant $t(76.6) = 3.02$, $p = 0.003$. Levene's Test for Equality of Variances did not allow assumptions for equal variances ($F = 10.48$, $p = 0.002$).

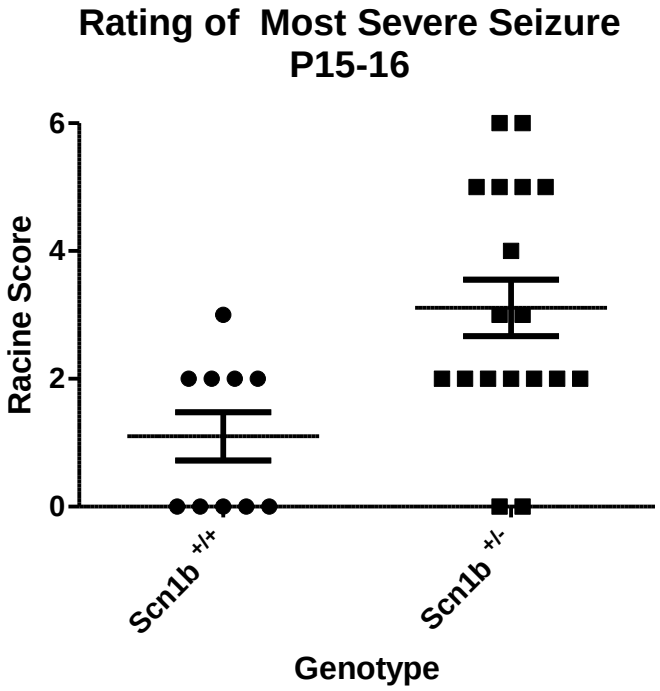

Figure 4: Ratings of the most severe seizures observed in P15-16 *Scn1b*$^{+/-}$ (*n* = 18) and *Scn1b* $^{+/+}$ mice (*n* = 10). *Scn1b*$^{+/-}$ mice (*Mdn* = 1.00, *SD* = 1.88) exhibited more severe seizures than *Scn1b* $^{+/+}$ mice (*Md n*= 2.50, *SD* = 1.20), (*U* = 37.0, *p* = 0.009)

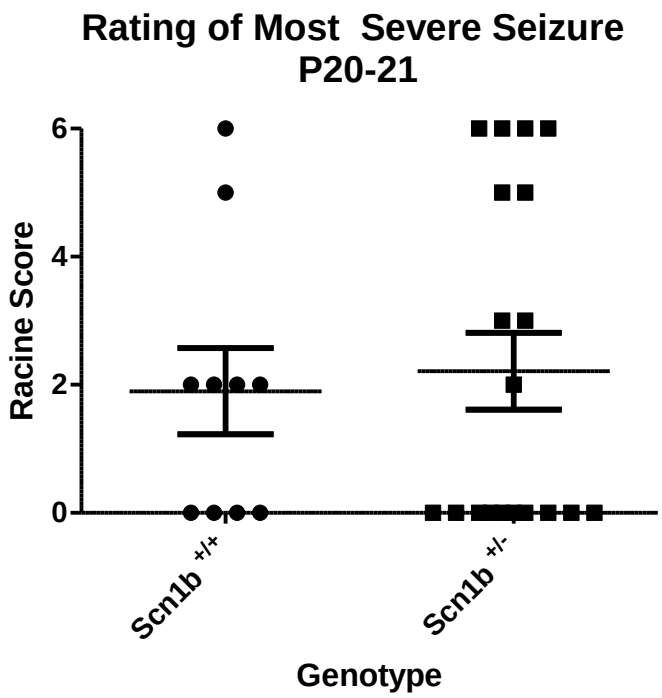

Figure 5: Ratings of the most severe seizures observed in P20-21 *Scn1b*$^{+/-}$ (*n* = 19) and *Scn1b*$^{+/+}$ mice (*n* = 10). There was no significant difference in seizure severity between *Scn1b*$^{+/-}$ (*Mdn* = 0.00, *SD* = 2.62) and *Scn1b*$^{+/+}$ mice (*Mdn* = 2.00, *SD* = 2.13), (*U* = 93.0, *p* = 0.94).

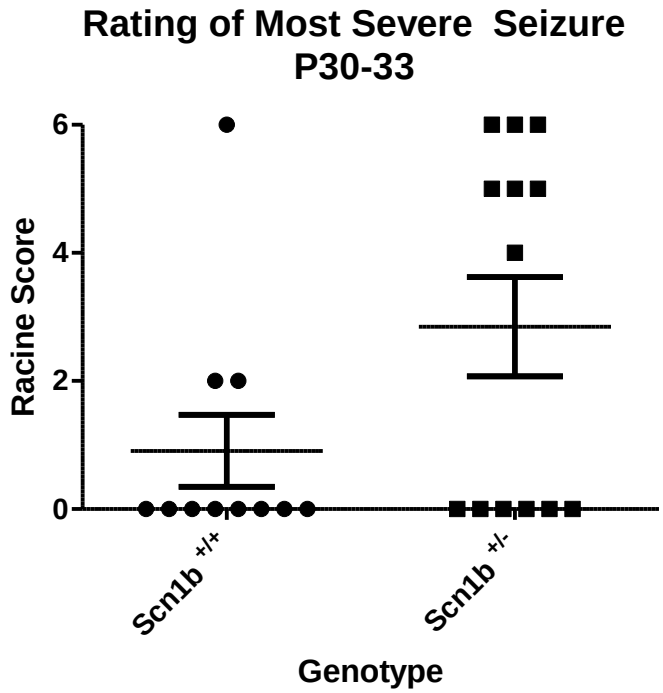

Figure 6: Ratings of the most severe seizures observed in P30-33 *Scn1b*$^{+/-}$ (*n* = 13) and *Scn1b*$^{+/+}$ (n = 11) mice. There was no significant difference in seizure severity between *Scn1b*$^{+/-}$ (*Mdn* = 4.00, *SD* = 2.79) and *Scn1b*$^{+/+}$ mice (*Mdn* = 0.00, *SD* = 1.87), (*U* = 47.5, *p* = 0.13).

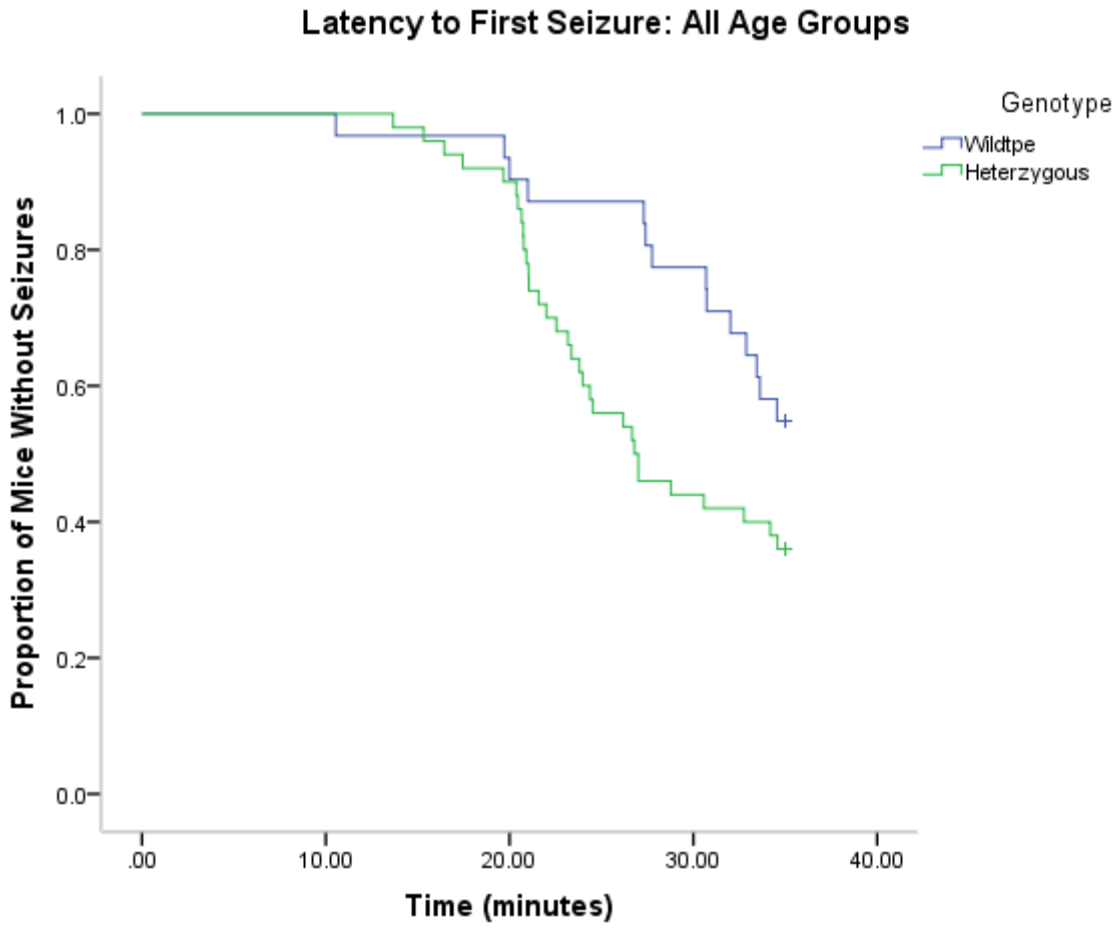

Figure 7: Survival curve function depicting latency to first seizure for *Scn1b*$^{+/-}$ (n = 50) and *Scn1b*$^{+/+}$ (n = 31) mice. *Scn1b*$^{+/-}$ mice had a greater probability of seizing earlier in the experimental period (M = 27.7 minutes, SE = 0.96) compared to *Scn1b*$^{+/+}$ mice (M = 31.5 minutes, SE = 1.07). The Mantel-Cox test indicated that differences in the survival distributions between *Scn1b*$^{+/-}$ and *Scn1b*$^{+/+}$ mice were significant (X^2 = 4.28, df = 1, p = 0.039).

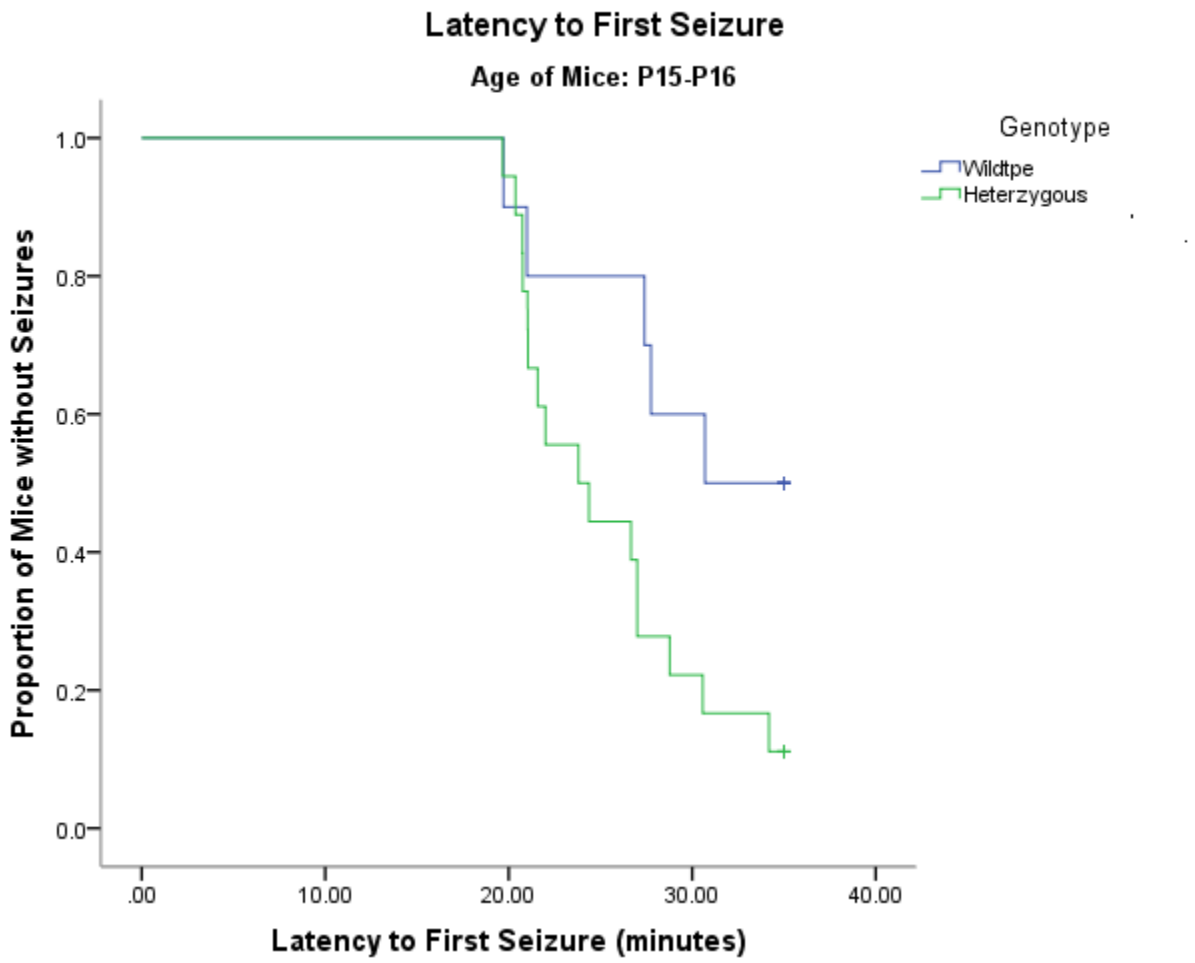

Figure 8. Survival curve function depicting latency to first seizure for P15-16 *Scn1b*$^{+/-}$ (n = 15) and *Scn1b*$^{+/+}$ (n = 10) mice. *Scn1b*$^{+/-}$ mice had a greater probability of seizing earlier into the experimental period (*M* = 25.53 minutes, *SE* = 1.21) compared to *Scn1b*$^{+/+}$ mice (*M* = 30.16 minutes, *SE* = 1.80). The Mantel-Cox test indicated that difference in the survival function was significant (X^2= 4.79, *df* = 1, *p* = 0.029).

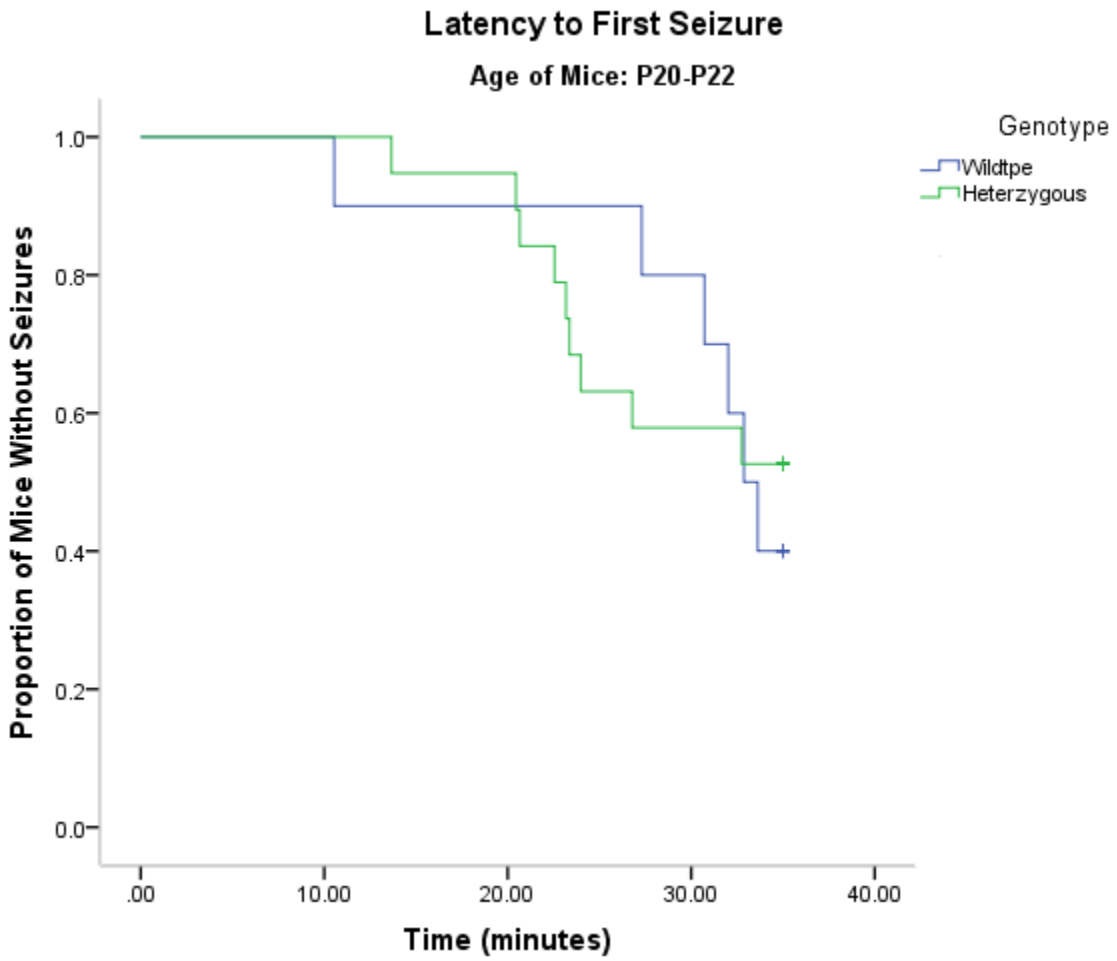

Figure 9. Survival curve function depicting latency to first seizure for P20-21 *Scn1b*$^{+/-}$ (n = 19) and *Scn1b*$^{+/+}$ (n = 10) mice. There was no significant difference in the latency to first seizure between *Scn1b*$^{+/-}$ (M = 29.34 minutes, SE = 1.57) and *Scn1b*$^{+/+}$ mice (M= 30.71 minutes, SE = 2.25). The Mantel-Cox test confirmed that the survival function did not differ between the two groups (X^2= 0.039, df = 1, p = 0.84).

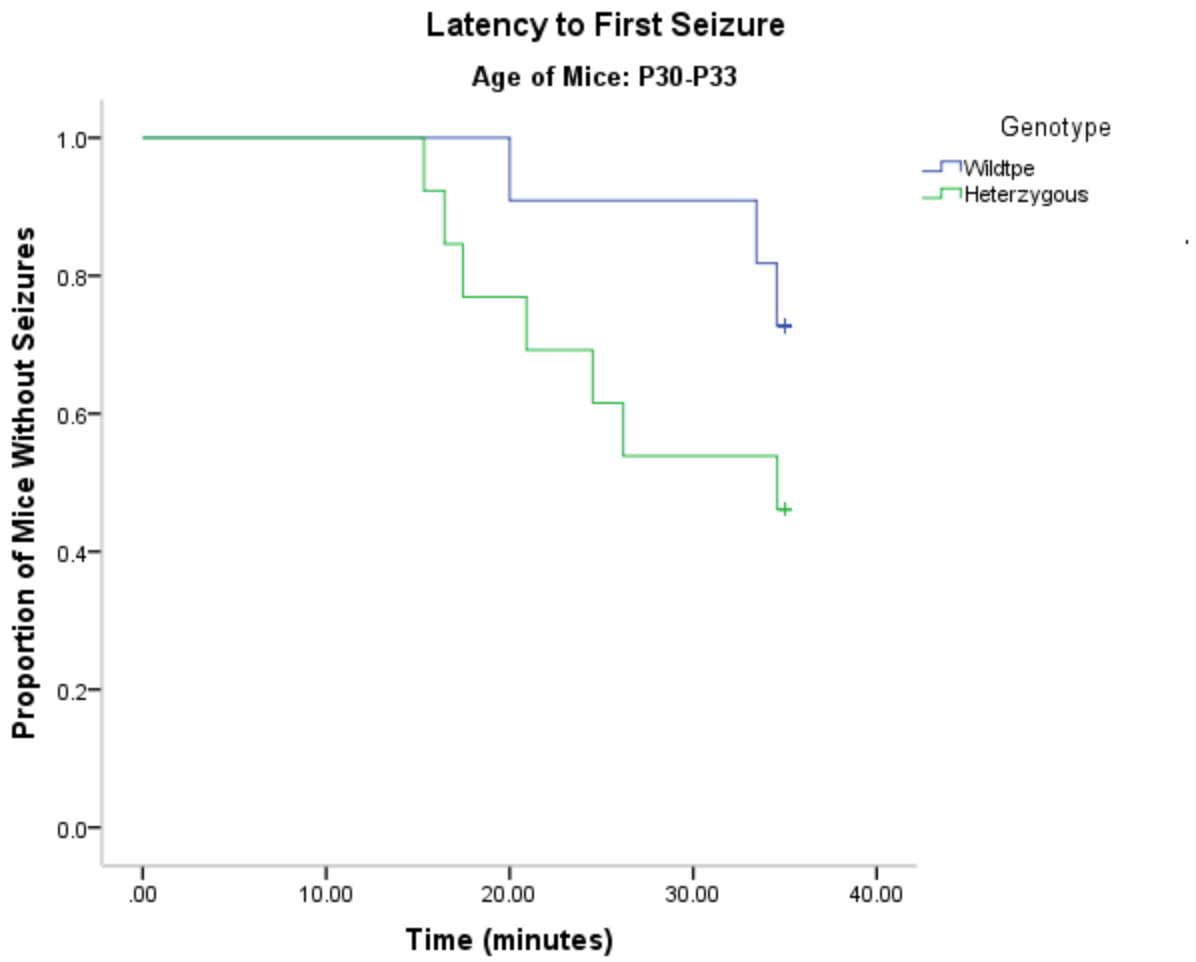

Figure 10. Survival curve function depicting latency to first seizure for P30-33 *Scn1b*$^{+/-}$ (n = 13) and *Scn1b*$^{+/+}$ (n = 11) mice. There was no significant difference in latency to first seizure between *Scn1b*$^{+/-}$ (M = 28.11 minutes, SE = 2.19) and *Scn1b*$^{+/+}$ mice (M = 33.46 minutes, SE = 1.29). The Mantel-Cox test confirmed that the survival function did not differ between the two groups (X^2 = 1.998, df = 1, p = 0.157)

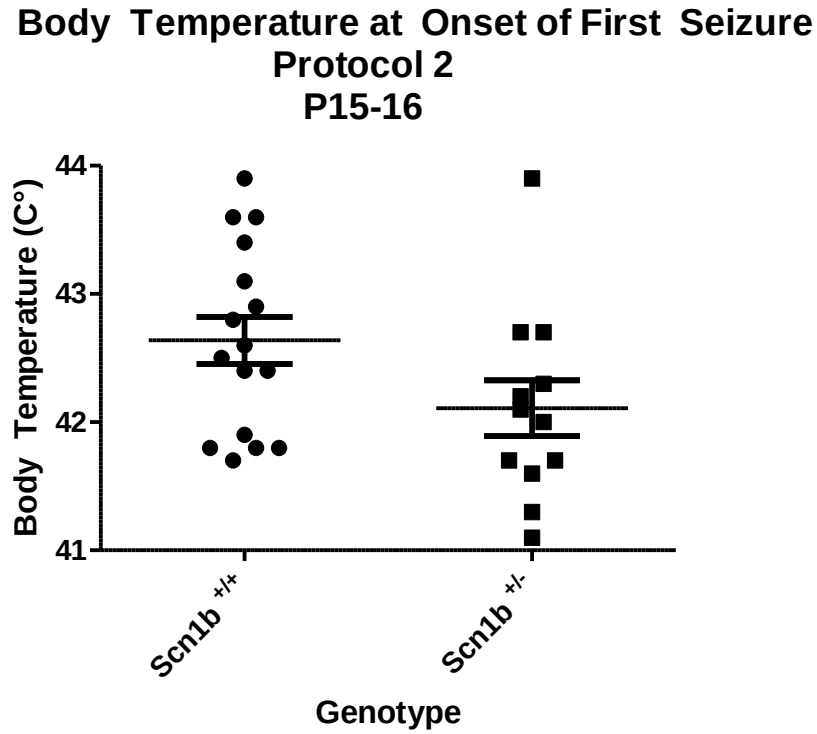

Figure 11. Core body temperature at onset of first seizure in P15-16 *Scn1b*$^{+/+}$ (*n* = 16) and *Scn1b*$^{+/-}$mice (*n* = 12) using the accelerated febrile seizure induction protocol (Protocol 2). *Scn1b*$^{+/+}$ mice (*Mdn* = 42.55°C, *SD* = 0.730) seized at a higher core body temperature than *Scn1b*$^{+/-}$ mice on average (*Mdn* = 42.05 °C, *SD* = 0.753) with little significance (*U* = 54.5, *p* = 0.057). However, a significant difference was found in core body temperature between *Scn1b*$^{+/+}$ (*Mdn* = 42.64 °C, *SD* = 0.730) and *Scn1b*$^{+/-}$ mice (*Mdn* = 42.00°, *SD* = 0.522) when the highest rated data point was removed from the *Scn1b*$^{+/-}$ data set (*U* = 39.0, *p* = 0.017). Although this point did not pass Grubbs' test for outliers (*Z* = 2.41, *p* > 0.05), a trend towards significance can be still suggested by the data. Additional febrile seizure experiments are needed to confirm these findings.

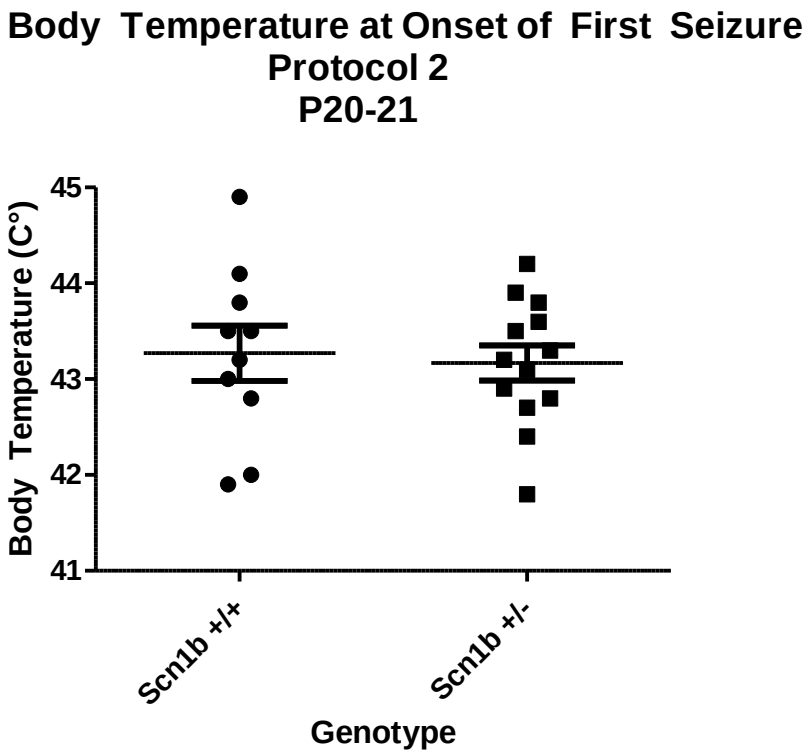

Figure 12. Core body temperature at onset of first seizure in P20-21 *Scn1b*$^{+/+}$ (*n* = 10) and *Scn1b*$^{+/-}$mice (*n* = 13) using the accelerated febrile seizure induction protocol (Protocol 2). There was no significant difference in core body temperature at onset of first seizure between *Scn1b*$^{+/+}$ (*Mdn*= 43.35°C, *SD*=0.914) and *Scn1b*$^{+/-}$ mice (*Mdn*= 43.20°C, *SD*=0.659) (*U*= 60.50, *p*=.804)

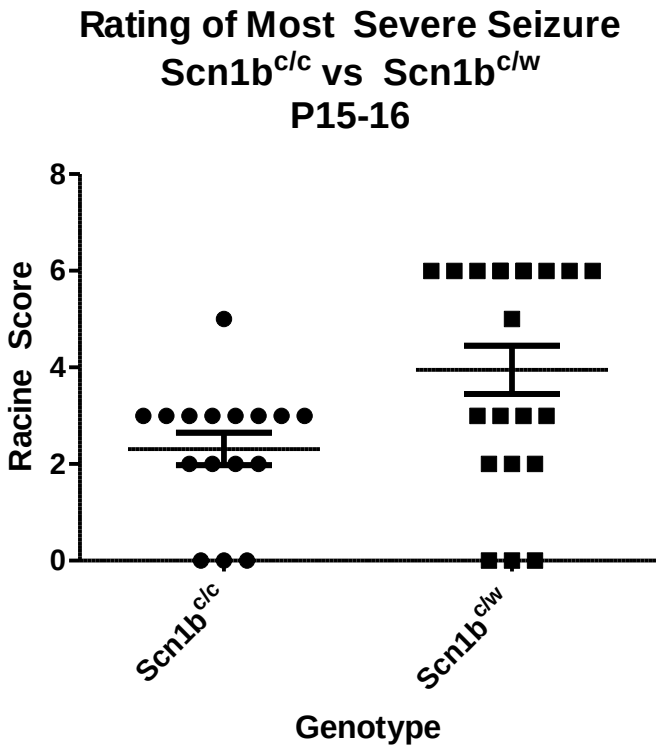

Figure13: Preliminary ratings of the most severe seizures observed in P15-16 *Scn1b*$^{c/c}$ (n = 16) and *Scn1b*$^{c/w}$ (n = 21) mice. Preliminary data suggest that *Scn1b*$^{c/w}$ mice (*Mdn* = 5.00, *SD* = 2.29) exhibited seizures of greater severity than *Scn1b*$^{c/c}$ mice (*Mdn* = 3.00, *SD* = 1.35), (*U* = 97.0, *p* = 0.026).

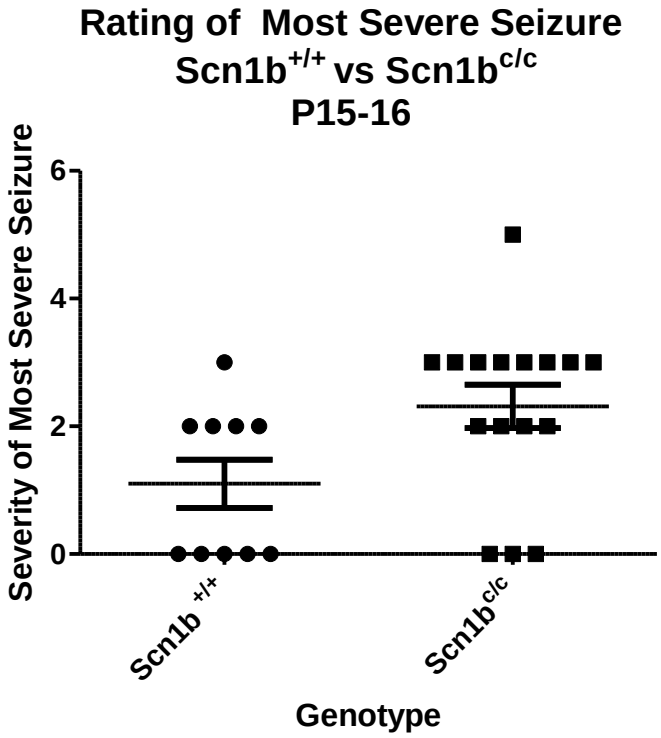

Figure 14: Ratings of most severe seizures observed in P15-16 *Scn1b*$^{+/+}$ (*n* = 10) and *Scn1b* $^{c/c}$ mice (*n* = 16). *Scn1b* $^{c/c}$ mice (*Mdn* = 3.00, *SD* = 1.35) exhibited seizures of greater severity than *Scn1b*$^{+/+}$ mice (*Mdn* = 1.00, *SD* = 1.20) (*U* = 38.50, *p* = 0.023).

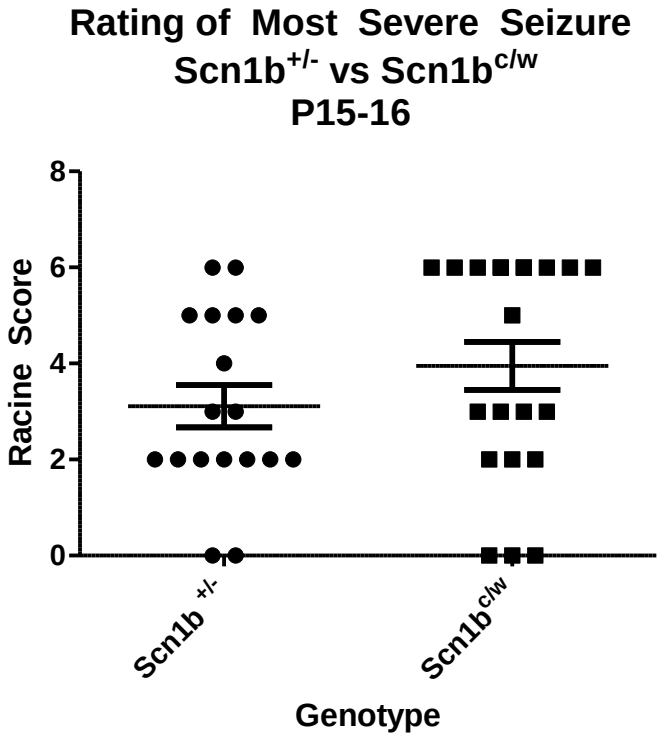

Figure 15: Ratings of most severe seizure observed in P15-16 *Scn1b*$^{+/-}$ (n = 18) and *Scn1b* $^{c/w}$ mice (n = 21). *Scn1b* $^{c/w}$ mice (*Mdn* = 5.00, *SD* = 2.29) and *Scn1b*$^{+/-}$ mice (*Mdn* = 2.50, *SD* = 1.88) did not differ significantly in their seizure severity ratings (U = 134.5, p = 0.12).

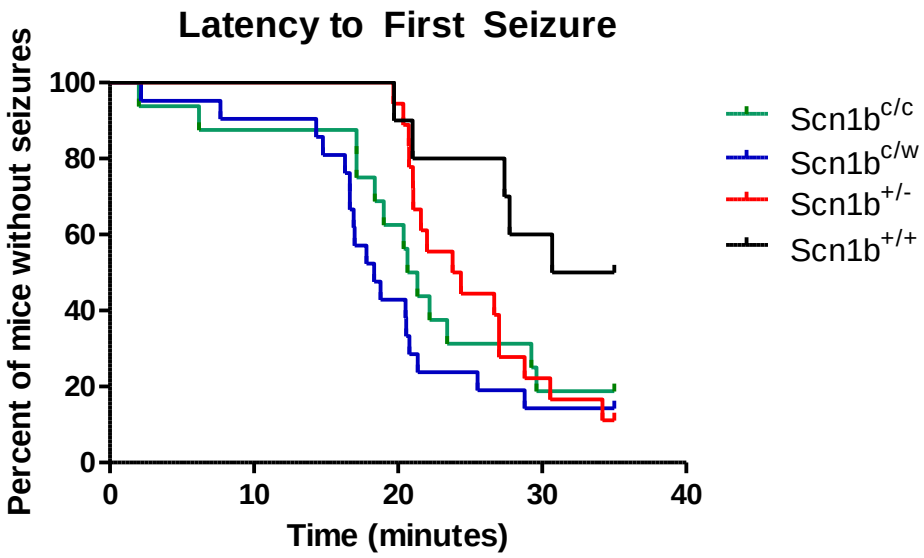

Figure 16: Survival function depicting latency to first seizure in P15-16 *Scn1b*$^{c/c}$ (n = 16), *Scn1b*$^{c/w}$ (*n* = 21) minutes, *Scn1b*$^{+/-}$ (*n* = 18) and *Scn1b*$^{+/+}$ (n = 10) mice. *Scn1b*$^{+/-}$ (*Mdn* = 24.09 minutes), *Scn1b*$^{c/c}$ (*Mdn* = 21.00 minutes), and *Scn1b*$^{c/w}$ (*Mdn* = 18.33 minutes) mice exhibited similar curves. *Scn1b*$^{+/+}$ mice (*Mdn* = 32.85 minutes) were the only group that seized later in the experimental period. The Mantel Cox Test confirmed that this difference was significant (X^2 = 9.41, *df* = 1, *p* = 0.024).